



A joint FTIR, FT-Raman and Scaled Quantum Mechanical study of 2', 4'-difluoro acetophenone and 4'-chloro acetophenone

N. Jayamani^{1,*} and N. Geetha²

¹Department of Physics, Vivekanandha College of Arts and Science (w), Namakkal-637205, India.

²Department of Chemistry, Bharathiyar Arts and Science College (w), Salem-636112, India.

ARTICLE INFO

Article history:

Received: 7 December 2012;

Received in revised form:

13 February 2013;

Accepted: 13 February 2013;

Keywords

2', 4'-difluoro acetophenone,
4'-chloro acetophenone,
Density functional theory,
FTIR; FT-Raman,
Vibrational spectra,
NMR chemical shifts.

ABSTRACT

This work deals with the vibrational spectroscopy of 2', 4'-difluoro acetophenone (DFA) and 4'-chloro acetophenone (CA). The fundamental vibrational frequencies and intensity of vibrational bands were evaluated using density functional theory (DFT) using standard B3LYP/6-31G** method and basis set combinations. The vibrational spectra were interpreted, with the aid of normal coordinate analysis based on a scaled quantum mechanical force field. The infrared and Raman spectra were also predicted from the calculated intensities. The effects of halogen substituents on the structure and vibrational frequencies have been investigated. Comparison of simulated spectra with the experimental spectra provides important information about the ability of the computational method to describe the vibrational modes. The ¹³C and ¹H NMR chemical shifts of the DFA and CA molecules were calculated using the Gauge-Invariant- atomic orbital (GIAO) method in DMSO solution using IEF-PCM model and compared with experimental data.

© 2013 Elixir All rights reserved.

1. Introduction

Acetophenone is a simplest aromatic ketone. It can be obtained by air oxidation of ethyl benzene, as a by-product of cumene. It occurs naturally in many foods including apple, cheese, apricot, banana and cauliflower. Commercially significant resins are produced from treatment of acetophenone with formaldehyde and base. The resulting polymers are components of coatings, adhesives and inks. Acetophenone is a raw material for the synthesis of some pharmaceuticals and is also listed as an approved excipient by the U.S. FDA. Acetophenone is used to create fragrances that correspond to almond, cherry, honeysuckle, jasmine and strawberry. Being prochiral, acetophenone is also a popular test substrate for asymmetric transfer hydrogenation experiments [1]. Derivatives of acetophenone form the base for conducting polymer also [2]. It is used as a polymerization catalyst for the manufacture of olefins. It is also used as an intermediate for pharmaceuticals, agrochemicals and other organic compounds. It is used in medicine; it was marketed as a hypnotic and anticonvulsant under the brand name hypnone. It was considered to have superior sedative effects than both paraldehyde and chloral hydrate. In human, acetophenone is metabolized to benzoic acid, carbonic acid and acetone. Chloro acetophenone is primarily used as a riot-control agent (tear gas) and in Chemical Mace [3-6]. It is also used as a pharmaceutical intermediate and formerly as an alcohol denaturant [3].

In the present investigation a complete study of vibrational spectra of 2', 4'-difluoro acetophenone (DFA) and 4'-chloro acetophenone (CA) have been carried out. The fluorine and bromine substituents present in the title compounds are highly electronegative and hence they withdraw the electrons from the ring, which results into the change in ionization potential, electronic affinity and excitation energies of the system.

The assignments of bands in the vibrational spectra of molecules are an essential step in the application of vibrational spectroscopy for solving various structural chemical problems. The philosophy of computational methods of vibrational spectroscopy changed significantly after the introduction of scaled quantum mechanical calculations (SQM) [7-9]. The vibrational analyses of DFA and CA using the SQM force field method based on DFT calculations have been presented [10]. The calculated infrared and Raman spectra of the title compounds were also simulated utilizing the scaled force fields and the computed dipole derivatives for IR intensities and polarizability derivatives for Raman intensities.

2. Experimentation

The compounds under investigation namely 2', 4'-difluoro acetophenone (DFA) and 4'-chloro acetophenone (CA) were kindly provided by the Sigma chemical company (U.S.A) and used as such for the spectral measurements. The room temperature Fourier transform infrared spectra of the title compounds were measured with KBr pellet technique in the 4000-400 cm⁻¹ region at a resolution of ±cm⁻¹ using BRUKER IFS 66V FTIR spectrometer equipped with a cooled MCT detector for the mid-IR range. Boxcar apodization is used for the 250 averaged interferograms collected for the sample and background.

The FT-Raman spectra are recorded on a BRUKER IFS-66V model interferometer equipped with an FRA-106 FT-Raman accessory. The spectra are recorded in the 4000-50 cm⁻¹ Stokes region using 1064 nm line of a Nd:YAG laser for excitation operating at 200 mW power. The reported frequencies are believed to be accurate within ±cm⁻¹. ¹H and ¹³C NMR spectra are taken in DMSO solutions and all signals are referenced to TMS on a BRUKER TPX-400 FT-NMR

spectrometer. All NMR spectra are measured at room temperature.

3. Computational details

Quantum chemical density functional calculations are carried out for DFA and CA with the 2003W version of the Gaussian suite programme [11] using the Becke-3-Lee-Yang-Parr(B3LYP) functionals [12-14] supplemented with the standard 6-31G** basis set (referred as DFT calculations). The normal grid (50,194) was used for numerical integration. The 6-31G** basis set adds polarization function in form of six d-type functions for each atom other than H to the split valence 6-31G basis. The Cartesian representation of the theoretical force constants has been computed at the fully optimized geometry by the assumption that both the molecules belong to C_s point group symmetry. The theoretical DFT force field is transformed from Cartesian into local internal coordinates and then scaled empirically according to the SM procedure [15-17].

$$F_{ij}^{Scaled} = (C_i C_j)^{\frac{1}{2}} F_{ij}^{B3LYP} \dots\dots\dots 1$$

where C_i is the scale factor of coordinate i , F_{ij}^{B3LYP} is the B3LYP/6-31G** force constant in the local internal coordinates,

and F_{ij}^{Scaled} is the scaled force constant. The transformation of force field from Cartesian to internal local-symmetry coordinates, the scaling [18,19], the subsequent normal coordinate analysis calculation of total energy distribution (TED) and prediction of IR and Raman intensities are done on a PC with the version V7.0-G77 of the MOLVIB programme written by Sundius [20-22]. To achieve, a close agreement between the observed and calculated frequencies, least square fit refinement algorithm is used. The force field obtained by this way is then used to recalculate the normal modes, TED's and the corresponding theoretically expected IR and Raman intensities to predict the full IR and Raman spectra. For the plots of simulated IR and Raman spectra, pure Lorentzian band shapes are used with a band width (FWHM) of 10 cm^{-1} .

For NMR calculations ^{13}C and ^1H NMR chemical shifts (δ_{H} and δ_{C}) are calculated using the GIAO method [23] in chloroform (CDCl₃) at B3LYP method with 6-31G** basis set. Relative chemical shifts are then estimated by using the corresponding TMS shielding calculated in advance at the same theoretical level as the reference. ^{13}C and ^1H isotropic magnetic shielding (IMS) of any X carbon (or hydrogen) atoms is made according to the value ^{13}C IMS of TMS: $\text{CS}_X = \text{IMS}_{\text{TMS}} - \text{IMS}_X$ (^1H IMS of TMS: $\text{HS}_X = \text{IMS}_{\text{TMS}} - \text{IMS}_X$). The experimental values for ^1H and ^{13}C isotropic chemical shifts for TMS were 13.84 and 188.1ppm, respectively [24].

The prediction of Raman intensities was carried out by following the procedure outlined below. The Raman activities (S_i) calculated by the GAUSSIAN-03 programme are adjusted during scaling procedure with MOLVIB were converted to relative Raman intensities (I_i) using the following relationship derived from the basic theory of Raman scattering [25-27].

$$I_i = \frac{f(\nu_o - \nu_i)^4 S_i}{\nu_i \left[1 - \exp\left(\frac{-h\nu_i}{KT}\right) \right]} \dots 2$$

Where ν_o is the exciting frequency (in cm^{-1} units), ν_i is the vibrational wave number of the i^{th} normal mode, h , c , and k are the universal constants and f is a suitably chosen common normalization factor for all peak intensities.

4. Results and discussion

4.1 Molecular structure and symmetry

The labeling of atoms of the title compounds are shown in Figs. 1 (a) and (b). The global minimum energies obtained by the DFT structure optimization of DFA and CA were found to be -583.370 and -844.502 Hartrees for B3LYP/6-31G** basis set, respectively. This energy difference is clearly understandable, since the molecules are under different chemical environments. Both DFA and CA belong to C_s point group symmetry.

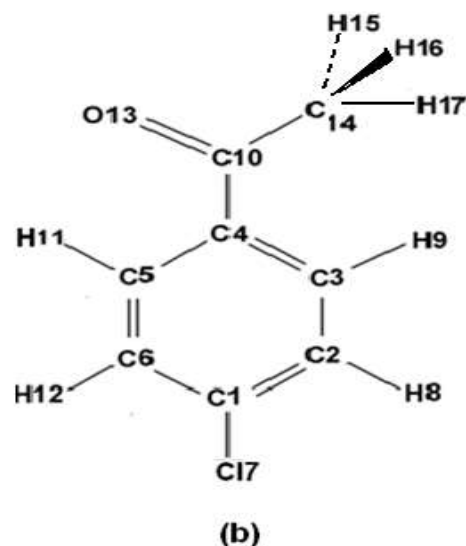
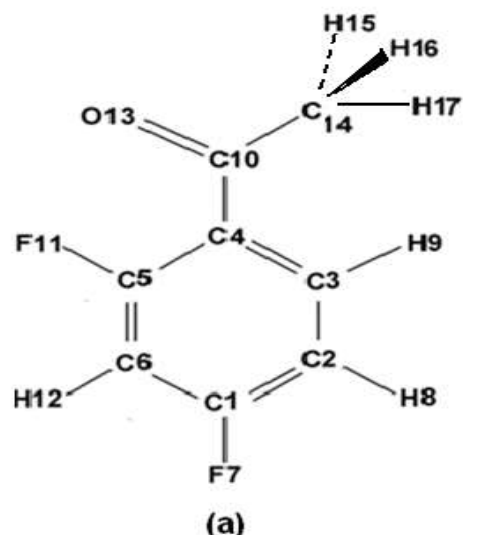


Fig.1 Molecular structure of

(a) 2', 4'-difluoro acetophenone along with numbering of atoms

(b) 4'-chloro acetophenone along with numbering of atoms

The 45 normal modes of DFA and CA are distributed among the symmetry species as

$$\Gamma_{\text{vib}} = 31A' \text{ (in-plane)} + 14A'' \text{ (out-of-plane)}$$

where A' and A'' irreducible representations correspond to in-plane and out-of-plane vibrations. All the vibrations are active both in the Raman scattering and infrared absorption. All the vibrational frequencies calculated using the optimized geometry was found to be positive for the title compounds. Bond lengths and bond angles calculated using DFT method for the title compounds are shown in Table 1. The fluorine and chlorine substitution in the benzene ring are highly electro negative and hence withdraw the electrons from the ring. As a result, the bond

length of carbon-hydrogen atoms in DFA and FA is very much shorter than C-F and C-Cl bond lengths. The presence of heavy fluorine atoms in the title compound (DFA) at second and fourth position of the ring significantly changes the bond length.

4.2 Vibrational Force Constant

The output files of the quantum-mechanical calculations contain the force constant matrix in Cartesian coordinates and in Hartree/Bohr² units. These force constants were transformed to the force fields in the internal local-symmetry coordinates. The local-symmetry coordinates, defined in terms of the internal valence coordinates following the IUPAC recommendations [28, 29] are given in Table 2 for DFA and CA, respectively. The force fields determined were used to calculate the vibrational potential energy distribution (PED) among the normal coordinates. The most important diagonal force constants of DFA and CA are listed in Table 2.

The bonding properties of DFA and CA are influenced by the rearrangements of electrons during substitutions and addition reactions. The values of the stretching force constants between carbon atoms in DFA and CA are found to be less than their characteristic values, since fluorine and chlorine are more electronegative and hence the bonded electrons between the carbon atoms are slightly shifted towards the halogen atoms of the title compounds. The values of the stretching force constants between carbon and fluorine atoms of DFA are found to be higher than the values of stretching force constant between carbon and chlorine atoms. Similarly, the values of the stretching force constants between carbon and fluorine atoms of DFA are found to be higher than the values of stretching force constant between carbon and hydrogen atom, since chlorine are less electronegative than fluorine atom.

4.3 Molecular Vibrations and Theoretical Prediction of Spectrum

The 45 normal vibrations of DFA and CA modes are distributed as 31 inplane vibrations and 14 out of plane vibrations in agreement with C_s symmetry. All vibrations were found to be active both in infrared absorption and Raman scattering. In the Raman spectrum the in-plane vibrations give rise to polarized bands while the out-of-plane gives to depolarized band. The observed and calculated infrared and Raman spectra of DFA and CA are produced in a common frequency scales in Figs. 2-5. The assignments of the normal modes of vibrations of the investigated molecules along with the observed fundamentals, unscaled frequencies obtained by B3LYP/6-31G** calculations and scaled frequencies as well as the PED descriptions are reported in Tables 3 and 4 for DFA and

CA respectively. Root mean square (RMS) values were obtained in this study using the following expression,

$$\text{RMS} = \sqrt{\frac{1}{(n-1)} \sum_i^n (\nu_i^{\text{calc}} - \nu_i^{\text{exp}})^2} \quad \dots 4.3$$

Deviations between the unscaled and experimental frequencies for all modes were found to be 30.2 cm⁻¹ and 35.3 cm⁻¹ for DFA and CA, respectively. This is quite obvious; since the frequencies calculated on the basis of quantum mechanical force fields usually differ appreciably from the observed frequencies. This is partly due to the neglect of anharmonicity and partly due to the approximate nature of the quantum mechanical methods. In order to reduce the overall deviation between the unscaled and observed fundamental frequencies, scale factors were applied in the normal coordinate analysis and the subsequent least square fit refinement resulted into a very close agreement between the observed fundamentals and the scaled frequencies (Table 3 and 4). Refinement of the scaling factors applied in this study achieved a weighted mean deviation of 10.4 cm⁻¹ and 9.7 cm⁻¹ between the experimental and SQM frequencies of the title compounds.

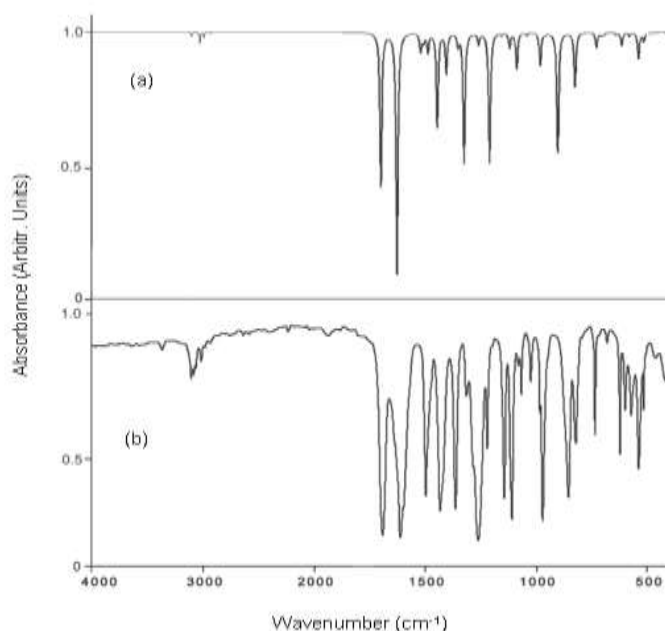


Fig. 2 Comparison of observed and calculated FTIR spectra of 2', 4' – difluoro acetophenone
a) calculated with B3 LYP/6-31G**
b) observed with KBr disc

Table 1. Optimized geometrical parameters of 2', 4'-difluoro acetophenone (DFA) and 4'-chloro acetophenone(CA) obtained by B3LYP6-31G density functional calculations.**

Bond length	Value(A°)		Bond angles	Value(°)	
	DFA	CA		DFA	CA
C1-C2	1.393	1.396	C1-C2-C3	118.159	118.971
C2-C3	1.387	1.389	C2-C3-C4	122.313	120.993
C3-C4	1.407	1.403	C3-C4-C5	116.618	118.869
C4-C5	1.401	1.402	C4-C5-C6	122.980	120.852
C5-C6	1.389	1.393	C6-C1-F7(C17)	118.545	119.313
C1-F7(C17)	1.343	1.755	C1-C2-H8	119.798	120.020
C2-H8	1.083	1.084	C2-C3-H9	120.934	120.834
C3-H9	1.084	1.084	C3-C4-C10	117.453	118.091
C4-C10	1.504	1.500	C4-C5-F11(H11)	120.395	120.454
C5-F11(H11)	1.350	1.084	C5-C6-H12	120.871	120.910
C6-H12	1.082	1.084	C4-C10-O13	119.213	120.429
C10-O13	1.221	1.221	C4-C10-C14	120.311	118.938
C10-C14	1.514	1.518	C10-C14-H15	110.952	111.097
C14-H15	1.094	1.095	C10-C14-H16	110.952	111.097
C14-H16	1.094	1.095	C10-C14-H17	108.279	108.651
C14-H17	1.090	1.090			

For numbering of atoms refer figs. 1(a) and (b).

Table 2. Definition of local symmetry coordinates and diagonal force constants of 2, 4 -difluoro acetophenone (DFA) and 4'-chloro acetophenone (CA)

No.	Symmetry coordinates ^a	Description		Diagonal force constants ^b	
		DFA	CA	DFA	CA
1	$S_1=r_{1,2}$	$\nu C1C2$	$\nu C1C2$	6.88	6.67
2	$S_2=r_{2,3}$	$\nu C2C4$	$\nu C2C43$	7.15	6.98
3	$S_3=r_{3,4}$	$\nu C3C4$	$\nu C3C4$	6.51	6.52
4	$S_4=r_{4,5}$	$\nu C4C5$	$\nu C4C5$	6.74	6.55
5	$S_5=r_{5,6}$	$\nu C5C6$	$\nu C5C6$	7.01	6.83
6	$S_6=r_{6,1}$	$\nu C6C1$	$\nu C6C1$	7.07	6.75
7	$S_7=r_{1,7}$	$\nu C1F7$	$\nu C1C17$	5.76	3.51
8	$S_8=r_{2,8}$	$\nu C2H8$	$\nu C2H8$	5.22	5.19
9	$S_9=r_{3,9}$	$\nu C3H9$	$\nu C3H9$	5.22	5.20
10	$S_{10}=r_{4,10}$	$\nu C4C10$	$\nu C4C10$	4.41	4.37
11	$S_{11}=r_{5,11}$	$\nu C5F11$	$\nu C5H11$	5.51	5.17
12	$S_{12}=r_{6,12}$	$\nu C6H12$	$\nu C6H12$	5.27	5.20
13	$S_{13}=r_{10,13}$	$\nu C10O13$	$\nu C10O13$	11.18	11.39
14	$S_{14}=r_{10,14}$	$\nu C10C14$	$\nu C10C14$	4.14	3.99
15	$S_{15}=r_{14,15}$	$\nu C14H15$	$\nu C14H15$	4.81	4.79
16	$S_{16}=r_{14,16}$	$\nu C14H16$	$\nu C14H16$	4.81	4.79
17	$S_{17}=r_{14,17}$	$\nu C14H17$	$\nu C14H17$	4.94	4.98
18	$S_{18}=\beta_{1,2,3}+\beta_{2,3,4}-2\beta_{3,4,5}+\beta_{4,5,6}+\beta_{1,6,5}-2\beta_{6,1,2}$	$\delta Ring1$	$\delta Ring1$	1.20	1.42
19	$S_{19}=\beta_{1,2,3}-\beta_{2,3,4}+\beta_{3,4,5}-\beta_{4,5,6}+\beta_{1,6,5}-\beta_{6,1,2}$	$\tau Ring2$	$\tau Ring2$	1.03	1.54
20	$S_{20}=\beta_{12,3}-\beta_{2,3,4}+\beta_{4,5,6}-\beta_{1,6,5}$	$\tau Ring3$	$\tau Ring3$	1.10	1.23
21	$S_{21}=\beta_{6,1,7}-\beta_{2,1,7}$	$\delta C1F7$	$\delta C1C17$	0.87	0.66
22	$S_{22}=\beta_{1,2,8}-\beta_{3,2,8}$	$\delta C2H8$	$\delta C2H8$	0.49	0.51
23	$S_{23}=\beta_{2,3,9}-\beta_{4,3,9}$	$\delta C3H9$	$\delta C3H9$	0.51	0.50
24	$S_{24}=\beta_{3,4,10}-\beta_{5,4,10}$	$\delta C4C10$	$\delta C4C10$	1.18	0.98
25	$S_{25}=\beta_{4,5,11}-\beta_{6,5,11}$	$\delta C5F11$	$\delta C5H11$	1.02	0.53
26	$S_{26}=\beta_{5,6,12}-\beta_{1,6,12}$	$\delta C6H12$	$\delta C6H12$	0.46	0.51
27	$S_{27}=\beta_{4,10,13}$	$\delta C4C10O13$	$\delta C4C10O13$	3.73	2.30
28	$S_{28}=\beta_{4,10,14}$	$\delta C4C10C14$	$\delta C4C10C14$	3.27	2.14
29	$S_{29}=\beta_{10,14,15}$	$\delta C10C14H15$	$\delta C10C14H15$	0.48	0.43
30	$S_{30}=\beta_{10,14,16}$	$\delta C10C14H16$	$\delta C10C14H16$	0.48	0.43
31	$S_{31}=\beta_{10,14,17}$	$\delta C10C14H17$	$\delta C10C14H17$	0.53	0.48
32	$S_{32}=\beta_{15,14,16}$	$\delta H15C14H16$	$\delta H15C14H16$	0.47	0.45
33	$S_{33}=\beta_{16,14,17}$	$\delta H16C14H17$	$\delta H16C14H17$	0.48	0.46
34	$S_{34}=\beta_{15,14,17}$	$\delta H15C14H17$	$\delta H15C14H17$	0.48	0.46
35	$S_{35}=\gamma_{7,1,6,2}$	$\gamma C1F7$	$\gamma C1C17$	0.60	0.56
36	$S_{36}=\gamma_{8,2,1,3}$	$\gamma C2H8$	$\gamma C2H8$	0.33	0.42
37	$S_{37}=\gamma_{9,3,2,4}$	$\gamma C6H9$	$\gamma C6H9$	0.47	0.51
38	$S_{38}=\gamma_{10,4,3,5}$	$\gamma C4C10$	$\gamma C4C10$	0.46	0.34
39	$S_{39}=\gamma_{11,5,4,6}$	$\gamma C5F11$	$\gamma C5H11$	0.62	0.46
40	$S_{40}=\gamma_{12,6,5,1}$	$\gamma C6H12$	$\gamma C6H12$	0.30	0.42
41	$S_{41}=\tau_{3,4,10,13}-\tau_{5,4,10,13}$	$\tau C10O13$	$\tau C10O13$	0.91	1.08
42	$S_{42}=\tau_{3,4,10,14}-\tau_{5,4,10,14}$	$\tau C10C14$	$\tau C10C14$	0.83	0.85
43	$S_{43}=-\tau_{4,10,14,15}-\tau_{4,10,14,16}-\tau_{6,10,14,17}$	$\tau CH3$	$\tau CH3$	0.08	0.05
44	$S_{44}=\tau_{1,2,3,4}+\tau_{2,3,4,5}-2\tau_{3,4,5,6}+\tau_{4,5,6,1}+\tau_{5,6,1,2}-2\tau_{6,1,2,3}$	$\tau Ring1$	$\tau Ring1$	0.47	0.38
45	$S_{45}=\tau_{1,2,3,4}-\tau_{2,3,4,5}+\tau_{3,4,5,6}-\tau_{4,5,6,1}+\tau_{5,6,1,2}-\tau_{6,1,2,3}$	$\tau Ring2$	$\tau Ring2$	0.40	0.36
46	$S_{46}=-\tau_{1,2,3,4}-\tau_{2,3,4,5}+\tau_{4,5,6,1}-\tau_{5,6,1,2}$	$\tau Ring3$	$\tau Ring3$	0.35	0.27

For numbering of atoms reference Figs. 1(a) and (b); Abbreviations: ν : stretching; δ : deformation in-plane; γ : deformation out-of-plane; τ : torsion.

^adefinitions are made in terms of the standard valence coordinates: r_{ij} is the bond length between atoms i and j; $\beta_{i,j,k}$ is the valence angle between atoms i,j,k where j is the central atom; $\gamma_{i,j,k,l}$ is the out-of-plane angle between the i-j bond and the plane defined by the j,k,l atoms; $\tau_{i,j,k,l}$ is the torsional (dihedral) angle between the plane defined by i,j,k and j,k,l atoms.

^bStretching force constants are given in mdyn \AA^{-1} , being and torsion force constants are given in mdyn \AA° .

Table 3. Detailed assignment of fundamental vibrations of 2', 4'-difluoro acetophenone (DFA) by normal mode analysis based on SQM force field calculations

Sl. No	Symmetry species	Observed frequencies (cm ⁻¹)		Calculated frequencies B3LYP/6-31G** force field cm ⁻¹		IR Intensity	Raman Activity	Characterization of normal modes with PED (%)
		FT IR	Raman	Unscaled	scaled			
1	A'	3100	-	3241	3101	0.350	118.484	νCH(99)
2	A'	-	3095	3232	3092	4.240	133.938	νCH(99)
3	A'	3078	-	3220	3080	0.360	36.286	νCH(99)
4	A'	3010	-	3172	3013	11.720	88.637	CH3ips(100)
5	A'	2950	-	3127	2971	6.031	48.198	CH3ss(100)
6	A''	-	2934	3061	2908	0.951	115.923	CH3ops(100)
7	A'	1690	-	1774	1690	152.915	27.116	νCO(61), bCC(13), νCC(11)
8	A'	1611	-	1666	1618	230.563	79.195	νCC(70), bCH(14)
9	A'	1597	-	1637	1603	44.670	6.789	νCC(72)
10	A'	-	1512	1534	1505	31.985	6.942	νCC(47), bCH(40)
11	A'	1497	-	1489	1497	8.982	20.791	CH3ipb(95)
12	A''	-	1480	1480	1479	19.559	9.940	CH3opb(91)
13	A'	1433	-	1465	1439	106.595	4.129	νCC(49), bCH(17)
14	A'	-	1404	1405	1404	33.736	5.905	CH3sb(38), CH3ipb(38)
15	A'	1363	-	1370	1355	14.510	1.158	νCC(82)
16	A'	1316	-	1314	1305	192.668	25.222	νCC(53), bCO(17), bCH(10)
17	A'	1261	-	1289	1263	89.235	11.429	νCF(36), νCC(27), bCH(26)
18	A'	1220	-	1245	1222	23.627	4.820	bCH(43), νCC(22), νCF(16)
19	A'	1144	-	1176	1142	12.226	2.713	bCH(57), νCC(18), νCF(17)
20	A'	1109	-	1133	1117	48.843	8.138	bCH(43), νCC(27), νCF(20)
21	A'	1067	-	1084	1065	36.744	12.489	Rtrigd(33), νCC(29), νCF(714)
22	A''	1024	-	1052	1035	2.874	1.552	CH3opr(73)
23	A'	983	-	993	971	16.103	6.564	CH3ipr(36), νCC(30), bCO(14)
24	A'	-	970	991	953	78.333	4.436	νCF(33), νCC(32), Rtrigd(12), bCH(10)
25	A''	864	-	976	879	5.790	0.516	ωCH(88)
26	A''	822	-	846	794	2.759	0.698	tRtrig(59), ωCH(14), ωCF(12)
27	A''	-	738	836	741	14.094	2.999	ωCH(51), tRtrig(31), ωCF(12)
28	A''	736	-	751	733	33.407	3.065	ωCH(63), tRtrig(24)
29	A'	-	684	703	718	10.286	16.857	νCC(37), νCF(17), Rasynd(17), bCO(10)
30	A'	632	-	687	682	2.854	2.713	νCC(39), Rtrigd(19), bCCm(11)
31	A''	623	-	633	624	10.098	0.045	tRasynd(39), ωCF(38)
32	A'	601	-	604	615	7.233	3.215	bCO(28), νCC(25), bCF(19)
33	A''	573	-	582	566	2.694	0.717	tRasynd(38), ωCF(26), tCO(16)
34	A'	539	-	546	538	9.416	3.375	bCCm(21), bCF(17), Rasynd(15), bCC(15)
35	A'	-	519	523	498	3.309	4.064	Rasynd(49), bCCm(13), νCF(11)
36	A''	464	-	465	463	0.615	0.362	tRsym(49), ωCF(26), tRasynd(11)
37	A'	-	398	399	406	3.204	0.925	bCF(37), bCCm(36), bCO(12)
38	A'	-	330	337	328	2.062	3.107	Rasynd(30), bCF(24), bCCm(18), νCC(15)
39	A''	-	320	322	311	0.021	2.761	ωCF(20), tRasynd(20), tRsym(19), tCO(13), tCC(12), ωCC(10)
40	A'	-	300	299	301	3.601	1.240	bCF(50), Rasynd(27), νCO(13)
41	A''	-	230	231	231	0.488	2.749	ωCF(46), tRasynd(18), ωCH(15)
42	A'	-	200	209	198	5.032	0.042	bCC(84)
43	A''	-	180	186	180	0.290	0.079	tCH3(79), bCH(11)
44	A''	-	102	102	107	1.679	0.511	tCO(28), tRsym(21), tRasynd(16), ωCC(14), tCC(10)
45	A''	-	-	51	49	3.807	0.007	tCC(50), tCO(44)

Abbreviations; R, ring; ss, symmetric stretching; ass, antisymmetric stretching; ips, in-plane stretching;

ops-out-of-plane stretching; b, bending; sb, symmetric bending; ipb, in-plane bending; opb, out-of-plane bending; ipr, in-plane rocking; opr, out of plane rocking; d, deformation; sym, symmetric; asy, asymmetric; ω, wagging; t, torsion; trig, trigonal; s, stretching. Only contributions larger than 10% are given.

Table 4. Detailed assignment of fundamental vibrations of 4'-chloro acetophenone (CA) by normal mode analysis based on SQM force field calculations

Sl. No	Symmetry species	Observed frequencies (cm ⁻¹)		Calculated frequencies B3LYP/6-31G** force field cm ⁻¹		IR Intensity	Raman Activity	Characterization of normal modes with PED (%)
		FT IR	Raman	Unscaled	scaled			
1	A'	3091	-	3227	3085	2.221	170.371	νCH(99)
2	A'	3078	-	3224	3083	3.902	59.027	νCH(99)
3	A'	-	3073	3214	3073	0.165	52.462	νCH(99)
4	A'	3064	-	3206	3065	4.835	42.779	νCH(99)
5	A'	3006	-	3169	3023	10.126	105.024	CH3ips(100)
6	A'	2968	-	3110	2967	8.660	47.461	CH3ss(100)
7	A''	2924	-	3048	2907	2.585	112.862	CH3ops(100)
8	A'	1687	-	1780	1687	146.843	55.323	νCO(72)
9	A'	1649	-	1645	1623	120.892	178.779	νCC (65), bCH(20), Rsymd(12)
10	A'	1589	-	1620	1584	17.900	11.316	νCC(72), bCH(11)
11	A'	1518	-	1528	1501	12.111	3.078	bCH(57), νCC(39)
12	A'	1488	-	1492	1464	9.615	22.067	CH3ipb(95)
13	A''	1429	-	1482	1452	12.569	10.040	CH3opb(91)
14	A'	1397	-	1441	1407	29.411	3.026	νCC(50), bCH(41)
15	A'	1358	-	1397	1355	49.260	4.925	CH3sb(41), CH3ipb(37)
16	A'	1303	-	1348	1318	4.614	6.585	νCC(87)
17	A'	1288	-	1325	1300	0.944	0.965	bCH(78), νCC(17)
18	A'	1251	-	1286	1262	171.558	48.270	νCC(60), Rtrigd(11)
19	A'	1178	1178	1204	1182	13.424	7.423	bCH(76), νCC(21)
20	A'	1107	-	1136	1113	7.629	0.692	bCH(61), νCC(21)
21	A'	-	1095	1109	1099	120.179	18.151	νCC(30), Rtrigd(29), νCCl(24), bCH(10)
22	A'	1076	-	1094	1068	2.710	30.845	νCC(55), CH3ipb(16), Rtrigd(13)
23	A'	-	1047	1048	1045	12.892	1.725	Rtrigd(41), νCC(40), bCH(18)
24	A''	1013	-	1028	1015	1.497	2.065	CH3opr(63), ωCH(18)
25	A''	968	-	996	965	0.787	0.496	ωCH(88)
26	A''	-	960	966	936	0.114	1.131	ωCH(85)
27	A'	930	-	963	932	33.384	7.713	CH3ipr(41), νCC(36)
28	A''	829	-	855	830	13.662	3.757	ωCH(92)
29	A''	-	785	836	813	30.037	0.999	ωCH(85)
30	A'	762	-	773	778	14.494	19.732	νCC(45), Rsymd(34), νCCl(14),
31	A''	713	-	726	715	0.205	0.023	tRtrig(72), ωCCl(10)
32	A'	-	632	643	632	1.057	6.478	Rasymd(85)
33	A'	622	-	626	615	4.794	1.717	νCCl(38), bCO(21), νCC(16)
34	A''	588	-	597	587	8.560	0.849	ωCC(25), tCO(23), tRtrig 12), ωCH(11)
35	A'	525	-	527	516	31.836	1.336	bCO(45), νCCl(20), νCC(16)
36	A''	470	-	476	471	3.173	0.117	tRasym(46), ωCCl(26)
37	A'	-	444	444	437	4.018	1.072	bCC(51), bCO(15)
38	A''	-	420	420	418	0.919	0.017	tRsym(43), tRasym(27), ωCH(13), ωCCl(10)
39	A'	-	311	317	307	0.409	4.792	Rsymd(32), νCC(27), νCCl(17)
40	A'	-	262	300	281	0.413	0.241	bCCl(50), bCC(22)
41	A''	-	250	259	241	0.098	1.596	ωCCl(45), ωCC(21), tRsym(14)
42	A'	-	170	173	163	3.999	0.651	bCC(44), bCCl(28), bCC(12), bCO(10)
43	A''	-	150	158	150	0.259	0.019	tCH3(81)
44	A''	-	88	89	83	2.211	0.175	tCO(33), tCC(18), tRsym(15), ωCC(14), ωCH(10)
45	A''	-	67	68	67	1.856	1.343	tCC(51), tCO(45)

Abbreviations; R, ring; ss, symmetric stretching; ass, antisymmetric stretching; ips, in-plane stretching; ops-out-of-plane stretching; b, bending; sb, symmetric bending; ipb, in-plane bending; opb, out-of-plane bending; ipr, in-plane rocking; opr, out of plane rocking; d, deformation; sym, symmetric; asy, asymmetric; ω, wagging; t, torsion; trig, trigonal; s, stretching. Only contributions larger than 10% are given.

Table 5. Atomic charges for optimized geometry of DFA and CA

Atoms ^a	B3LYP/6-31G**	
	Mulliken	
	DFA	CA
C1	0.370245	-0.08959
C2	-0.136915	-0.071807
C3	0.107741	-0.095043
C4	-0.011200	0.047803
C5	0.31170	-0.117570
C6	-0.195836	-0.075332
F7(Cl7)	-0.284679	-0.008294
H8	0.114432	0.117819
H9	0.137228	0.129235
C10	0.401731	0.396246
F11(H11)	-0.287049	0.098462
H12	0.124594	0.115396
O13	-0.452886	-0.451578
C14	-0.384063	-0.400725
H15	0.127147	0.124438
H16	0.132127	0.139324
H17	0.141735	0.141217

^aThe atoms indicated in the parenthesis belongs to CA; for numbering of atoms refer Figs 1 (a) and (b).

Table 6. Theoretically computed energies (a.u), zero-point vibrational energies (kcal/mol), rotational constants (GHz), entropies (cal/mol-kelvin) and dipolemoment (Debye).

Parameters	B3LYP/6-311+G**	
	DFA	CA
Total energy	-583.371	-844.502
Zero-point energy	76.388	80.586
Rotational constant	2.217	3.673
	0.752	0.550
	0.564	0.480
The virial (-V/T)	2.008	2.006
Entropy		
Total	95.729	94.460
Translational	41.044	41.005
Rotational	30.214	30.184
Vibrational	24.471	23.270
Dipole moment	1.743	2.323

Table 7. HOMO – LUMO energy value calculated by B3LYP/6-31G**

Parameters (a.u)	B3LYP/6-311+G**	
	DFA	CA
HOMO	-0.284	-0.270
LUMO	0.192	0.205
HOMO -LUMO	-0.092	-0.065

Table 8. Theoretical and experimental ¹H NMR and ¹³C NMR spectra of DFA and CA (with respect to TMS, all values in ppm) for B3LYP/6-31G**

Atoms	DFA		CA	
	Exp	Cal	Exp	Cal
C1	159.79	99.77	139.44	114.90
C2	131.62	133.80	128.84	142.12
C3	125.75	184.13	129.92	178.35
C4	134.62	135.07	135.54	161.11
C5	117.96	96.88	129.72	163.06
C6	156.43	109.74	128.84	140.76
C10	195.28	151.42	196.51	151.46
C14	26.30	44.21	26.40	39.69
H8	6.95	6.17	7.43	7.47
H9	7.94	7.20	7.88	6.41
H11	-	-	7.88	7.71
H12	6.87	5.10	7.43	7.53
H15	2.62	4.02	2.58	4.82
H16	2.62	4.02	2.58	4.82
H17	2.62	4.50	2.58	6.96

For numbering of atoms refer Figs 1 (a) and (b).

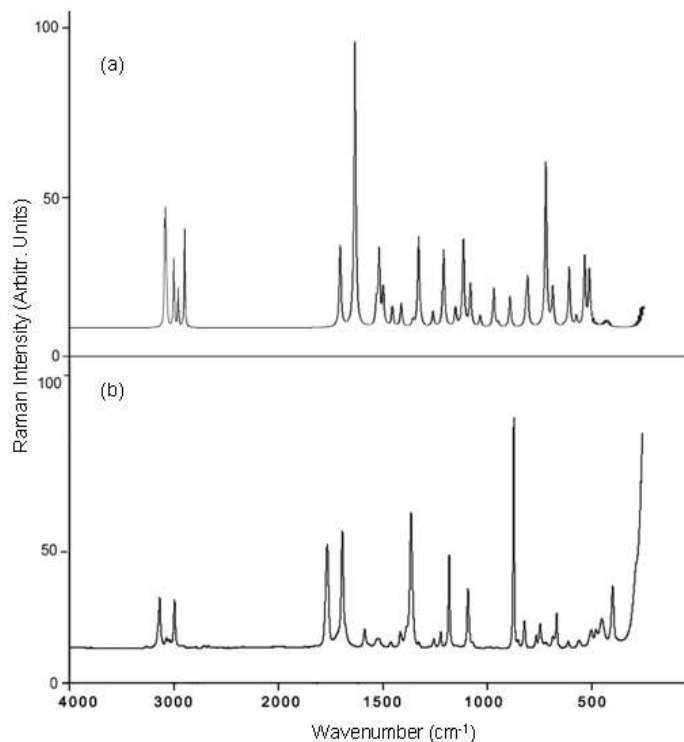


Fig.3 Comparison of observed and calculated FT-Raman spectra of 2', 4' – difluoro acetophenone
 a) calculated with B3 LYP/6-31G**
 b) observed with KBr disc

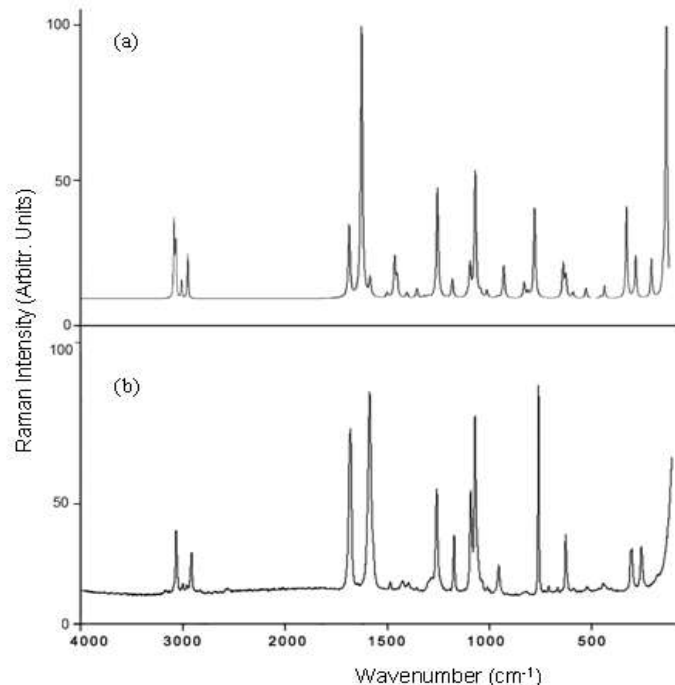


Fig.5 Comparison of observed and calculated FT-Raman spectra of 4' – chloro acetophenone
 a) calculated with B3 LYP/6-31G**
 b) observed with KBr disc

Due to the low symmetry of the molecule, several internal coordinates contribute to each normal mode of the title compounds. The detailed vibrational assignments of fundamental modes of DFA and CA by normal mode analysis based on scaled quantum mechanical force field calculations are listed in Tables 3 and 4.

5. Analysis of vibrational spectra

Density functional theory is known for the good performance in the estimation of vibrational spectra of organic compounds and it can be observed in the case of DFA and CA also. The unscaled B3LYP/6-31G** vibrational frequencies are generally larger than the experimental values. In order to obtain a reasonable frequency matching, scale factors proposed by Rauhut and Pulay [10] were employed. The scale factors were applied and optimized via least square refinement algorithm. The fundamental vibrational frequencies of various modes of vibrations are described below.

5.1 Methyl Group Vibrations

For the assignments of CH₃ group wavenumbers, basically nine fundamentals can be associated to each CH₃ group namely, CH₃ ss – symmetric stretch; CH₃ ips – in-plane stretch (i.e. in-plane hydrogen stretching modes); CH₃ ipb – in-plane bending (i.e. in-plane hydrogen deformation modes); CH₃ sb – symmetric bending; CH₃ ipr – in-plane rocking; CH₃ opr – out-of-plane rocking; tCH₃ – twisting hydrogen bending modes. In addition to that, CH₃ ops – out-of-plane-stretch and CH₃ opb – out-of-plane bending modes of CH₃ group would be expected to be depolarized for A symmetry species. The CH₃ ss wavenumbers are established at 2950 cm⁻¹ and 2968 cm⁻¹ in IR and CH₃ ips are assigned at 3010 cm⁻¹ and 3006 cm⁻¹ in IR for DFA and CA. These assignments are also supported by literature [30] in addition to PED output.

The two in-plane methyl hydrogen deformation modes are also well established. We have observed the symmetrical methyl deformation modes CH₃ sb at 1404 cm⁻¹ in Raman and 1358 cm⁻¹

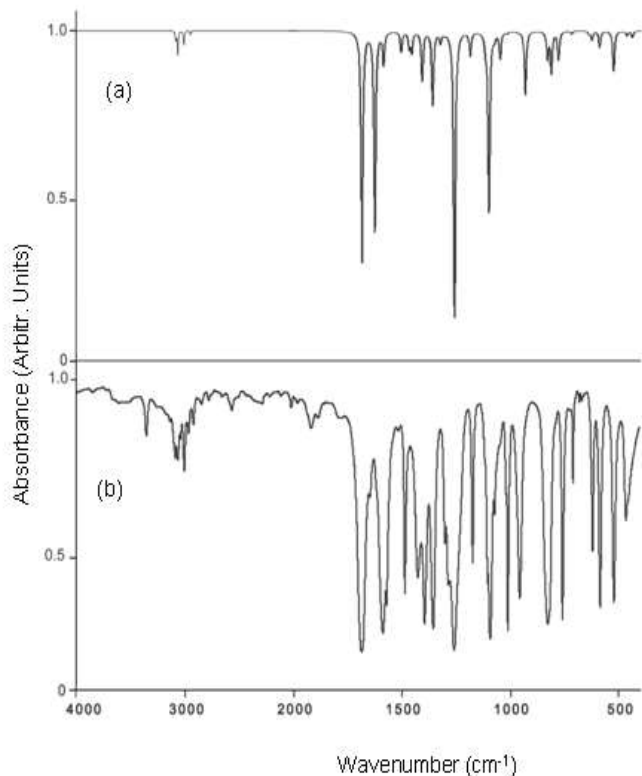
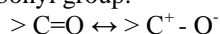


Fig.4 Comparison of observed and calculated FTIR spectra of 4' – chloro acetophenone
 a) calculated with B3 LYP/6-31G**
 b) observed with KBr disc

¹ in IR and in-plane methyl deformation modes CH₃ ipb at 1497 cm⁻¹ and 1488 cm⁻¹ in IR for DFA and CA. The bands at 2934 cm⁻¹ in Raman and 2924 cm⁻¹ in IR and 1480 cm⁻¹ in Raman and 1429 cm⁻¹ in IR are attributed to CH₃ ops and CH₃ ipb respectively in the A species. The methyl deformation modes mainly coupled with in-plane bending vibrations. The bands obtained at 983, 930 cm⁻¹ and 1024, 1013 cm⁻¹ in IR are assigned to CH₃ in-plane and out-of-plane rocking modes. The assignment of the bands at 180 cm⁻¹ and 150 cm⁻¹ in Raman are attributed to methyl twisting modes for DFA and CA.

5.2 Carbonyl Group Vibrations

The DFA and CA molecules are acquiring a highly polar bond containing carbon and oxygen which is formed by p_r-p_r between carbon and oxygen. Because of the different electronegativities of carbon and oxygen atoms, the bonding electrons are not equally distributed between the two atoms. The following two resonance forms contribute to the bonding of the carbonyl group.



The lone pair of electrons on oxygen also determines the nature of carbonyl group.

The carbonyl stretching modes identified at 1690 and 1687 cm⁻¹ in FTIR for DFA and CA [31, 32]. The FTIR bands identified at 601 and 525 cm⁻¹ are in-plane deformation and FT-Raman bands 102 and 88 cm⁻¹ are out-of-plane deformation for the carbonyl group respectively and are supported by the literature [33].

5.3 Carbon-Hydrogen Vibrations

Aromatic compounds commonly exhibit multiple weak bands in the region 3100 – 3000 cm⁻¹ due to aromatic C-H stretching vibrations [31, 34]. The title compound DFA has three C-H moieties. The vibrational wavenumbers assigned to the aromatic C-H stretching computed as 3101, 3092 and 3080 cm⁻¹ by B3LYP method shows good agreement with the recorded FTIR and FT-Raman bands at 3100, 3095, and 3078 cm⁻¹ [35]. The CA has four C-H stretching modes and show weak IR bands observed at 3091, 3078 and 3064 cm⁻¹ and FT-Raman bands are observed at 3073 cm⁻¹. All the aromatic C-H stretching bands are found to be weak, and this is due to a decrease of the dipole moment caused by reductions of negative charge on the carbon atom. This reduction occurs because of the electron withdrawal on the carbon atom by the different electronegative substituents such as –COCH₃, F and Cl due to inductive effect [36, 37]. The C-H in-plane bending vibrations are usually weak and observed in 1300-1000 cm⁻¹ region. The C-H out-of-plane bending modes are observed in the region 900-600 cm⁻¹ [38]. In the present work, the bands observed at 1220, 1144 and 1109 cm⁻¹ in DFA and 1397, 1288, 1178 and 1107 cm⁻¹ in CA were assigned to C-H in-plane bending vibrations. The C-H out-of-plane bending modes for DFA and CA were assigned within characteristic region [39] and are reported in Tables 3 and 4.

5.4 C-X Vibrations (Where X=F, Cl)

Strong characteristic absorptions due to the C-X stretching vibrations are observed in this study. The ring stretching, in-plane and out-of-plane bending vibrations have been identified and presented in Tables 3 and 4 for the title compounds. They are also supported by the literature [39, 40]. In the organic halogen compounds the band due to C-F stretching vibrations may be found over a wide wavenumber range, 1400 – 1000 cm⁻¹, since the vibration is easily influenced by adjacent atoms or groups. The vibrations belonging to the bond between the ring and the halogen atoms are worth to discuss here, since mixing of

vibrations are possible due to the lowering of the molecular symmetry and the presence of heavy atoms on the periphery of the molecules [41]

Bonds between atoms of higher masses will vibrate at lower wavenumbers than the bonds bearing the lighter atoms. In DFA very strong and the medium strong FTIR bands at 1261 cm⁻¹ and FT-Raman band at 970 cm⁻¹ are assigned to CF stretching.

The C-Cl stretching vibrations give generally strong bands in the region 760-505 cm⁻¹ [31, 41]. In the present study, the strong band observed in Raman spectrum at 522 cm⁻¹ was assigned to C-Cl stretching mode of CA.

In general, the assignments proposed for DFA is in agreement with the results proposed by Meric Bakiler et al., [41] and George Socrates [31].

5.5 Other molecular properties

(a) Charge analysis

Atomic charges of DFA and CA have been calculated by DFT method shown in Table 5. The magnitude of the carbon atomic charges is found to be positive and negative. The magnitude of the hydrogen atomic charges is found to be only positive and is arranged in an order from 0.114 to 0.141 for DFA and 0.117 to 0.141 for CA.

(b) Thermodynamic properties

Several thermo dynamical parameters have been calculated by using DFT and 6-31G** basis set has been given in Table 6. Scale factors have been recommended for an accurate prediction determining the zero-point vibrational energies for DFT calculation. The total energy of the molecule is the sum of the translational, rotational, vibrational and electronic energies.

5.6 HOMO and LUMO analysis

Many organic molecules that contain conjugated π electrons are characterized as hyper-polarisabilities and are analyzed by means of vibrational spectroscopy [42, 43]. In most of the cases, even in the absence of an inversion center, the strongest bands in the Raman spectrum are weak in the IR spectrum and vice versa. But the intramolecular charge transfer from the donor to acceptor group through a single- double bond conjugated path can induce large variations of both the molecular dipole moment and the molecular polarisability, making IR and Raman activity strong at the same time. The experimental spectroscopic behavior described above is well accounted for by ab initio calculations in π -conjugated systems that predict exceptionally large Raman and infrared intensities for the same normal modes [43]. It is also observed in our title molecules that the bands in FTIR spectrum have their counterparts in the Raman which shows that the relative intensities in IR and Raman spectra are comparable and also explains the result from the electron cloud movement through π conjugated frame work from electron donor to acceptor groups. The analysis of the wave function indicates that the electron absorption corresponds to the transition from the ground to the first excited state and is mainly described by one-electron excitation from the highest occupied molecular orbital [HOMO] to the lowest unoccupied molecular orbital [LUMO]. The LUMO of π nature is delocalized over the whole C-C bond. By contrast, the HOMO is located over N and the lower part of the ring, consequently the HOMO \rightarrow LUMO transition implies an electron density transfer to H and the upper part of the ring. Moreover, these orbitals significantly overlap in their position for DFA and CA. The atomic orbital compositions of the Frontier molecular orbital are sketched in Figs. 6 and 7.

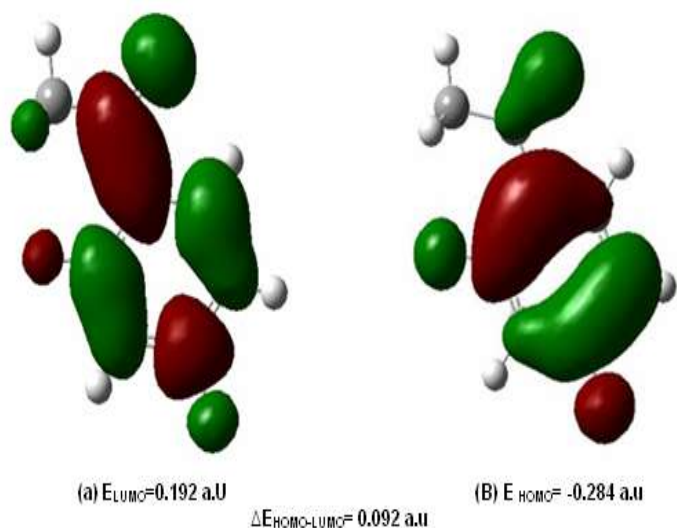


Fig. 6 HOMO and LUMO plot of 2', 4' – difluoro acetophenone

The HOMO – LUMO energy gap of DFA and CA have been calculated at the B3LYP/6-31G** level and are shown in Table 7, which reveals that the energy gap reflect the chemical activity of the molecules. LUMO is an electron acceptor

represents the ability to obtain an electron and HOMO represents the ability to donate an electron.

For DFA,

$$\text{HOMO energy} = -0.284 \text{ a.u.}$$

$$\text{LUMO energy} = 0.192 \text{ a.u.}$$

$$\text{HOMO – LUMO energy gap} = -0.092 \text{ a.u.}$$

For CA,

$$\text{HOMO energy} = -0.270 \text{ a.u.}$$

$$\text{LUMO energy} = 0.205 \text{ a.u.}$$

$$\text{HOMO – LUMO energy gap} = -0.065 \text{ a.u.}$$

The calculated self-consistent field (SCF) energy of DFA is -583.370a.u and CA is -844.502 a.u. Moreover, the lower HOMO and LUMO energy gap explains the eventual charge transfer interactions taking place within the molecules.

5.7 NMR spectra

The molecular structure of the title compounds is optimized. Then, gauge –including atomic orbital (GIAO) ^{13}C NMR and ^1H NMR chemical shifts calculations of the title compounds have been carried out by using B3LYP/ functional with 6-31G** basis set. The GIAO [44, 45] method is one of the most common approaches for calculating isotropic nuclear magnetic shielding tensors. The NMR spectra calculations were performed by using the Gaussian 03 [11] program package.

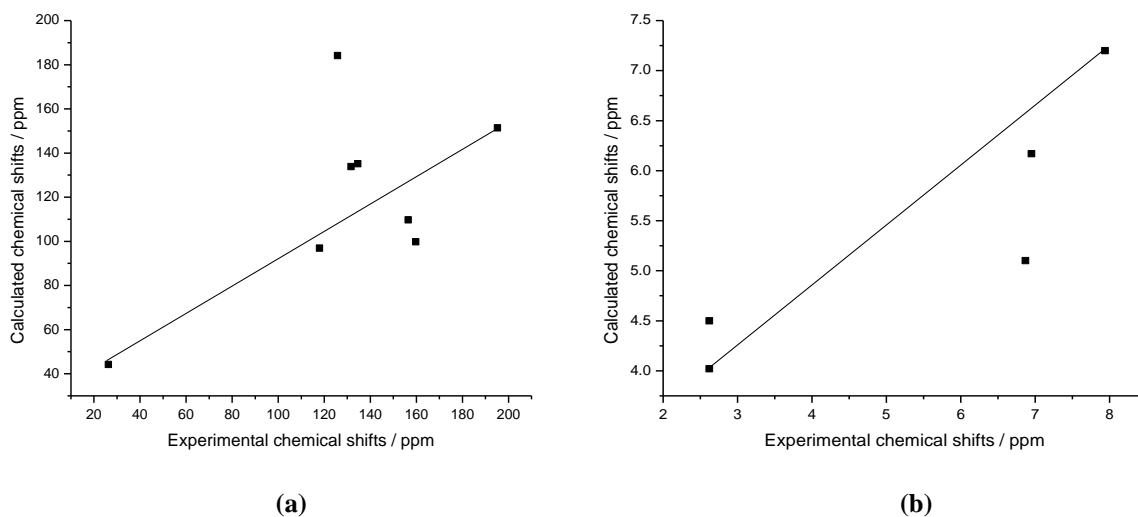


Fig. 8 The linear regression between experimental and theoretical ^{13}C (a) and ^1H (b) NMR chemical shifts for 2', 4'-difluoro acetophenone

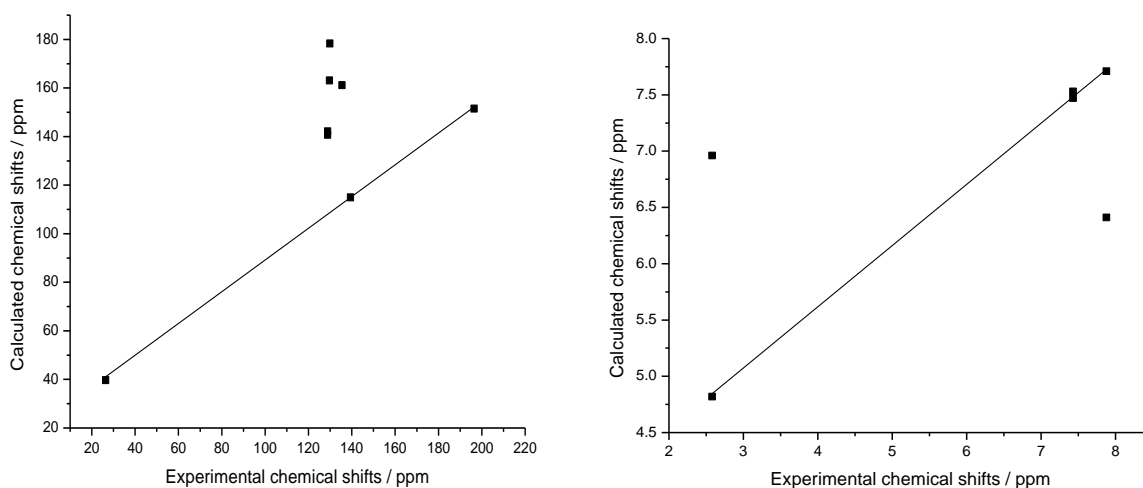


Fig. 9 The linear regression between experimental and theoretical ^{13}C (a) and ^1H (b) NMR chemical shifts for 4'-chloro acetophenone

Experimental and theoretical chemical shifts of DFA and CA in ^{13}C NMR and ^1H NMR spectra were recorded and the obtained data are presented in Table 8. The linear correlations between calculated and experimental data of ^{13}C NMR and ^1H NMR spectra are noted. Correlation coefficients of ^{13}C NMR and ^1H NMR are determined as 0.6225 and 0.9035 for DFA and 0.7724 and 0.7383 for CA. The data shows a good correlation between predicted and observed proton and carbon chemical shifts. The correlations of NMR spectra are presented in Figs. 8 and 9 for DFA and CA. The agreement between the experimental and calculated data is satisfactory for carbon-13 and slightly worse for proton shifts. The protons are located on the periphery of the molecule and therefore are supposed to be more susceptible to molecular (solute - solvent) effects than carbons.

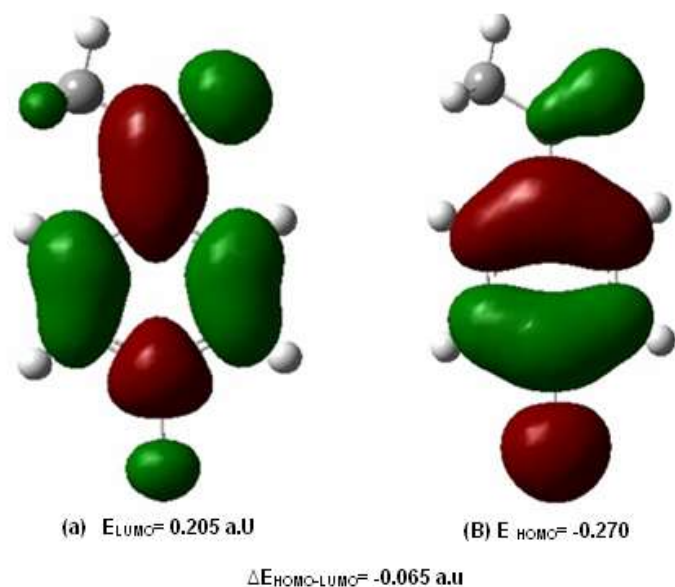


Fig. 7. HOMO and LUMO plot of 4'-chloro acetophenone

For this reason the agreement between the experimental and calculated data for protons is worse than that of carbon-13 [46].

The range of the ^{13}C NMR chemical shifts for a typical organic molecule usually is >100 ppm [47,48] and the accuracy ensures reliable interpretation of spectroscopic parameters. In the present study, the ^{13}C NMR chemical shifts in the ring for DFA and CA are >100 ppm, as they would be expected. The C14 atom in DFA and CA which bonds to methyl shows determined ^{13}C NMR shifts very low.

6. Conclusion

Based on the SQM force field obtained by DFT calculations at B3LYP/6-31G** level, a complete vibrational analysis of DFA and CA are performed. The fluorine and chlorine substitutions in the ring produced a remarkable effect on the geometric and spectroscopic properties of the title compounds. The -I > +M effect of the chlorine and fluorine acted not only on the close environment of the place of the substitution but also on other parts of the ring through π -electron system. As a result of the halogen atoms substituents in the ring, system makes remarkable changes were observed in the ring breathing modes, in-plane bending modes and out-of-plane bending modes of the title compounds. The theoretical calculations have allowed assign definitely the vibrational spectrum in low frequency region. In this region, there are several modes affected by the fluorine substitution of the aromatic ring. The assignment of

most of the fundamentals provided in the present work is believed to be unambiguous.

References

- [1] Prof. Dr. Christian A. Sandoval, Prof. Dr. Takeshi, Ohkuma, Noriyuki Utsumi, Kunihiko Tsupsumi, Dr. Kunihiko Murata, Prof. Dr. Ryoji Noyori, Chemistry, 1 (2006) 102-110.
- [2] J. Tarabek, E. Jahne, P. Rapta, D. Ferse, H. J. Adler and L. Dunsch, Russian Journal of Electro chemistry, 42 (2000) 1169-1176.
- [3] U.S. Department of Health and Human Services. Hazardous Substances Data Bank (HSDB, online database). National Toxicology Information Program, National Library of Medicine, Bethesda, MD. 1993.
- [4] The Merck Index. An Encyclopedia of Chemicals, Drugs, and Biologicals. 11th ed. Ed. S. Budavari. Merck and Co. Inc., Rahway, NJ. 1989.
- [5] National Toxicology Program. Toxicology and Carcinogenesis Studies of 2-Chloroacetophenone (CAS No. 532-27-4) in F344/N Rats and B6C3F₁ Mice (Inhalation Studies). TR No. 379. U.S. Department of Health and Human Services, Public Health Service, National Institutes of Health, Bethesda, MD. 1990.
- [6] M. Sittig. Handbook of Toxic and Hazardous Chemicals and Carcinogens 2nd ed. Noyes Publications, Park Ridge, NJ. 1985.
- [7] G. Forgarasi, P. Pulay, J.R. Durig, (Ed.), Vibrational Spectra and Structure, Elsevier, Amsterdam, 14 (1985) 125 (Chapter 3).
- [8] P. Pulay, H.F. Schaefer, III (Ed), Application of Electronic Structure Theory, Modern Theoretical Chemistry, Plenum, New York, 4 (1997) 153.
- [9] Y.N. Panchenko. J. Mol. Struct., 567 (2001) 217.
- [10] G. Rauhut, P. Pulay, J. Phys. Chem., 99 (1995) 3093.
- [11] M.J. Frisch, G.W. Trucks, H.B. Schlegel, G.E. Scuseria, M.A. Robb, J.R. Cheesman, V.G. Zakrzewski, J.A. Montgomery Jr., R.E. Stratmann, J.C. Burant, S. Dapprich, J.M. Millam, A.D. Daniels, K.N. Kudin, M.C. Strain, O. Farkas, J. Tomasi, V. Barone, M. Cossi, R. Cammi, B. Mennucci, C. Pomelli, C. Adamo, S. Clifford, J. Ochterski, G.A. Petersson, P.Y. Ayala, Cui, K. Morokuma, N. Roga, P. Salvador, J.J. Dannenberg, K. Malick, A.D. Rabuck, K. Rahavachari, J.B. Foresman, J. Cioslowski, J.V. Ortiz, A.G. Baboul, B.B. Stefanov, G. Liu, A. Liashenko, P. Piskorz, I. Komaromi, R. Gomperts, R.L. Martin, D.J. Fox, T. Keith, M.A. AL-Laham, C.Y. Peng, A. Nanayakkara, M. Challacombe, P.M.W. Gill, B. Johnson, W. Chen, M.W. Wong, J.L. Andres, C. Gonzalez, M. Head-Gordon, E.S. Replogle, J.A. Pople, Gaussian 03, Revision A 9, Gaussian, Inc., Pittsburgh PA, 2003.
- [12] A.D. Becke, J. Chem. Phys. 98 (1993) 5648-5652.
- [13] A.D. Becke, Phys. Rev. A 38 (1998) 3098.
- [14] P. Pulay, G. Forgarasi, F. Pong, J.E. Boggs, J. Am. Chem. Soc. 101 (1979) 2550-2560.
- [15] P. Pulay, G. Forgarasi, G. Pongor, J. E. Boggs, A. Vargha, J. Am. Chem. Soc. 105 (1983) 7037-7047.
- [16] G. Forgarasi, P. Pulay, J.R. Durig, (Ed.), Vibrational Spectra and Structure, Elsevier, Amsterdam, 14 (1985) 125 (Chapter 3).
- [17] P. Pulay, H.F. Schaefer, III (Ed), Application of Electronic Structure Theory, Modern Theoretical Chemistry, Plenum press, New York, 4 (1977) 153-185.
- [18] G. Forgarasi, X. Zhou, P.W. Taylor, P. Pulay, J. Am. Chem. Soc. 114 (1992) 8191-8201.
- [19] G. Rauhut, P. Pulay, J. Phys. Chem. 99 (1995) 3093-3100.
- [20] T. Sundius, J. Vib. Spectrosc. 874 (2002) 1.

- [21] T. Sundius, *Vibr. Spectrosc.* 29 (2002) 89-95. MOLVIB (V.7.0) Calculation of Harmonic Force Fields and Vibrational Modes of Molecules, CPE Program No. 807 (2002).
- [22] T. Sundius, MOLVIB: a program for harmonic force fields calculations, CPE Program No. 604, *J. Mol. Struct.* 218 (1990) 321-326.
- [23] K. Wolinski, J. F. Hinton, P. Pulay, *J. Phys. Chem. Soc.* 112 (1990) 8251.
- [24] J. R. Cheeseman, G. W. Trucks, T. A. Keith, M. J. Frisch, *J. Chem. Phys.* 104 (1996) 5497.
- [25] P.L. Polavarapu, *J. Phys. Chem.*, 94 (1990) 8106
- [26] G. Keresztury, S. Holly, J. Varga, G. Besenyeyi, A.Y. Wang, J.R. Durig, *Spectrochim. Acta Part A*, 49 (1993) 2007.
- [27] G. Keresztury, *Raman spectroscopy: Theory*, in *Handbook of Vibrational Spectroscopy*, J.M. Chalmers, P.R. Griffiths (edn), John Wiley & Sons, Ltd., 1 (2002) 71.
- [28] Y. Morino, T. Shimanouchi, IUPAC Commission on Molecular Structure on spectroscopy, *Pure. Appl. Chem.*, 50 (1978) 1707.
- [29] P. Pulay, G. Forgarasi, F. Pong, J.E. Boggs, *J. Am. Chem. Soc.*, 101 (1979) 2550.
- [30] S.J. Bunce, H.G. Edwards, A.F. Johnson, I.R. Lewis, P.H. Turler, *Spectrochim. Acta.*, 49A (1993) 775.
- [31] GeorgeSocrates, *Infrared and Raman Characteristic Group Frequencies – Tables and Charts*. Third ed., John Wiley & sons, New York. 2001
- [32] V. Krishna Kumar, V. Balachandran, *Spectrochim. Acta part A*, 61 (2005) 2510.
- [33] Mehmet Karavacak, Kurt Mustafa, *J.Mol.Structure.* 919 (2009) 215.
- [34] G. Varsanyi, *Assignments for Vibrational Spectra of 700 Benzene Derivatives*, 1 (1973) 433-434.
- [35] A. Kovacs, G. Keresztury, V. Izvekov, *Chem. Phys.* 193 (2000) 253.
- [36] D.N. Sathyanarayanan, *Vibrational Spectroscopy Theory and Application*, New Age International publishers, New Delhi, 2004.
- [37] J. Karpagan, N. Sundaraganesan, S. Sebastian, S .Manoharan, M. Kurt, *J. Raman spectrosc.*, 41 (2010) 53.
- [38] W.O. George, P.S. Cintyne, IN. D.J. Mowthrope (Ed.) *Infrared Spectroscopy*, John Wiley and Sons, UK 1987.
- [39] T.D. Klots, P. Devlin, W.B. Collier, *Spectrochim. Acta A*, 53 (1997) 2445.
- [40] V. Krishna Kumar, S. Muthunatesan. *Spectrochim. Acta Part A*, 66 (2007) 1082.
- [41] Meric Bakiiler, I.V. Maslov, Sevim Akyiiz, *J. Mol. Struct.*, 83 (1999) 475.
- [42] Y. Ataly, D. Avci, and A. BaSoglu, Linear and non-linear optical properties of some donor- acceptor oxadiazoles by ab initio Hartree Fock calculations, *Struct. Chem.* 19 (2008) 239-246.
- [43] C. James, C. Ravikumar, T. Sundius, V. Krishnakumar, R. Kesavamoorthy, V. S. Jayakumar, and I. Hubert Joe, FT-Raman and FT-IR spectra, normal coordinate analysis and ab initio computations of (2-methylphenoxy) acetic acid dimmer, *Vibrat. Spectros.* 47 (2008) 10-20.
- [44] R. Ditchfield, *J. Chem. Phys.* 56 (1972) 5688.
- [45] K. Wolinski, J. F. Hilton, P. Pulay, *J. Am. Chem. Soc.* 112 (1990) 8251.
- [46] B. Osmialowski, E. Kolehmainen, R. Gawinecki, *Magn. Reson. Chem.* 39 (2001) 334- 340.
- [47] H. O. Kalinowski, S. Berger, S. Barun, *C-13 NMR Spectroscopy*, John Wiley and Sons: Chichester, 1988.
- [48] K. Pihlaja, E. Kleinpeter (Eds), *Carbon-13 Chemical Shifts in Structural and Stereo Chemical Analysis*, VCH Publishers: Deerfield Beach, FL, 1994.